Available online at www.sciencedirect.com
SCIENCE DIRECT®
Journal of Solid State Chemistry 177 (2004) 515–522
JOURNAL OF SOLID STATE CHEMISTRY
http://elsevier.com/locate/jssc

The study of $Bi_3B_5O_{12}$: synthesis, crystal structure and thermal expansion of oxoborate $Bi_3B_5O_{12}$

Stanislav Filatov,[a,*] Yurij Shepelev,[b] Rimma Bubnova,[b] Natalia Sennova,[a] Anna V. Egorysheva,[c] and Yury F. Kargin[c]

[a] *Department of Crystallography, St. Petersburg State University, University Emb. 7/9, St. Petersburg 199034, Russia*
[b] *Grebenshchikov Institute of the Silicate Chemistry of the Russian Academy of Sciences, Ul. Odoevskogo 24 korp 2, St. Petersburg 199155, Russia*
[c] *Kurnakov Institute of General and Inorganic Chemistry of the Russian Academy of Sciences, Leninsky Prospect 31, GSP-1, Moscow 119991, Russia*

Received 27 September 2002; accepted 19 March 2003

Abstract

The paper presents a new data on the crystal structure, thermal expansion and IR spectra of $Bi_3B_5O_{12}$. The $Bi_3B_5O_{12}$ single crystals were grown from the melt of the same stoichiometry by Czochralski technique. The crystal structure of $Bi_3B_5O_{12}$ was refined in anisotropic approximation using single-crystal X-ray diffraction data. It is orthorhombic, *Pnma*, $a=6.530(4)$, $b=7.726(5)$, $c=18.578(5)$ Å, $V=937.2(5)$ Å^3, $Z=4$, $R=3.45\%$. Bi^{3+} atoms have irregular coordination polyhedra, $Bi(1)O_6$ (d(B–O) = 2.09–2.75 Å) and $Bi(2)O_7$ (d(B–O) = 2.108–2.804 Å). Taking into account the shortest bonds only, these polyhedra are considered here as trigonal $Bi(1)O_3$ (2.09–2.20 Å) and tetragonal $Bi(2)O_4$ (2.108–2.331 Å) irregular pyramids with Bi atoms in the tops of both pyramids. The BiO_4 polyhedra form zigzag chains along *b*-axis. These chains alternate with isolated anions $[B_2^{IV}B_3^{III}O_{11}]^{7-}$ through the common oxygen atoms to form thick layers extended in *ab* plane. A perfect cleavage of the compound corresponds to these layers and an imperfect one is parallel to the Bi–O chains. The $Bi_3B_5O_{12}$ thermal expansion is sharply anisotropic ($\alpha_{11}\approx\alpha_{22}=12$, $\alpha_{33}=3\times10^{-6}\,^{\circ}C^{-1}$) likely due to a straightening of the flexible zigzag chains along *b*-axis and decreasing of their zigzag along *c*-axis. Thus the properties like cleavage and thermal expansion correlate to these chains.

Keywords: $Bi_3B_5O_{12}$; Oxoborate; Bismuth borate; Crystal structure; Thermal expansion; Oxocentered polyhedra; Isolated boron–oxygen anion; IR spectroscopy

1. Introduction

Traditionally, borates are used for glass production. Nowadays excellent non-linear optical properties for β-BaB_2O_4, LiB_3O_5, CsB_3O_5, $CsLiB_6O_{10}$, $Ca_4GdO(BO_3)_3$ and $Ca_4YO(BO_3)_3$ [1–5], piezoelectricity for $Li_2B_4O_7$ [6] and/or laser properties have been found. The unique crystal structures of these borates determine their enhanced UV transparency, good non-linearity and relatively high resistance against laser induced damage. Bismuth borates are of a great interest for material scientists [7–16] as BiB_3O_6 was found to be a highly promising material for non-linear optics [7–9], high double-refraction was found for $Bi_4B_2O_9$ [10], stimulated Raman scattering [14] and luminescence properties [16] were found for $Bi_3B_5O_{12}$. Application of the new promising materials requires the knowledge of their crystal structure in correlation with physical properties. Information about thermal expansion is important for crystal growth and the use of crystals at elevated temperatures. It was shown [17] that borates mostly have highly anisotropic thermal expansion and the great average volume expansion about $60\times10^{-6}\,^{\circ}C^{-1}$. At the same time the results of the previous studies of two bismuth borates showed that their thermal expansion is comparatively low: it is equal to about $37\times10^{-6}\,^{\circ}C^{-1}$ [11,12].

The bismuth borate, $Bi_3B_5O_{12}$, was first described as a compound by Levin and McDaniel [18], crystal growth and cleavage of $Bi_3B_5O_{12}$ were investigated in Ref. [19]. The crystal structure of the compound was determined in isotropic approximation by Vegas et al. [20]: it crystallizes in orthorhombic space group *Pnma* with the

*Corresponding author.
E-mail address: filatov@crystal.pu.ru (S. Filatov).

0022-4596/$ - see front matter © 2003 Elsevier Inc. All rights reserved.
doi:10.1016/j.jssc.2003.03.003

following parameters $a = 6.532$, $b = 7.733$, $c = 18.566$ Å, $Z = 4$, $R = 9.7\%$. The title compound contains an additional oxygen not bonded to any boron–oxygen groups and situated in the centers of isolated OBi_3 triangles. The compound was attributed to oxoborates with a formula $Bi_3O(B_5O_{11})$. Recently, Raman spectra of $Bi_3B_5O_{12}$ were studied for the first time in Ref. [14]. In the present paper a novel data on crystal structure refinement in anisotropic approximation are given in correlation to IR- and Raman spectra and physical properties like the coefficients of thermal expansion and a cleavage. In contrast to the previous study using absorption corrections and a larger number of observed reflections the esds of atomic parameters were reduced in about 10 times [20].

Table 1
Crystal data

Parameters	293 K
Crystal dimensions	$0.14 \times 0.5 \times 0.13\,mm^3$
Symmetry	*Pnma*
a (Å)	6.530 (4)
b (Å)	7.726 (5)
c (Å)	18.578 (5)
V (Å^3)	937.2 (5)
Z	4
Total number of $F(h\,k\,l)$	1521
$F(h\,k\,l)$ with $I \geqslant 4(\sigma(I))$	1425
R-factor (1521 $F(h\,k\,l)$) (%)	4.50
R_w-factor (1521 $F(h\,k\,l)$) (%)	4.27
R-factor (1425 $F(h\,k\,l)$) (%)	3.80
R_w-factor (1425 $F(h\,k\,l)$) (%)	3.61
Sig1-factor	1.3

2. Experimental

2.1. Crystal growth

The $Bi_3B_5O_{12}$ single crystals were grown from the melt of the same stoichiometry by Czochralski technique with a resistance heated platinum crucible (about 90 cm^3). The starting charge was sintered of Bi_2O_3 (purity 99.999 mass%) and H_3BO_3 (purity 99.999 mass%) by a solid-state reaction for the purpose of the melt homogeneity. Seeds, oriented along [0 1 0] direction, were cut from a block crystal grown onto a platinum wire. Since borate melts tend to glass formation due to their high viscosity, the melt was cooled down at a rate not higher than 0.2°C/h, and the axial temperature gradient was kept within the limit of 0.8°C/cm. During the growth process, the highest pulling and rotation rates were at 1 mm/h and 8 rpm, accordingly.

The facetting of the crystals obtained is characterized by irregular hexagonal prisms and well-developed forms {1 0 1} and {0 0 1}. They have a perfect cleavage parallel to {0 0 1} and an imperfect one parallel to {1 0 0} as it was mentioned in Ref. [19]. The maximal size of the as-grown single crystal was about 17 mm in diameter and 40 mm in length.

2.2. Crystal structure refinement

The crystal of a prismatic shape (dimensions $0.14 \times 0.5 \times 0.13\,mm^3$) was mounted on the three-circle automatic diffractometer with the perpendicular beam scheme. The unit-cell parameters of $Bi_3B_5O_{12}$ (Table 1) were determined on a diffractometer using high order $h\,0\,0$, $0\,k\,0$ and $0\,0\,l$ reflections. Integrated intensities of the X-ray reflections were measured at room temperature. Graphite-monochromatized Mo$K\alpha$-radiation ($\lambda = 0.71069$ Å) and a perpendicular-inclination measurement technique were used. The stability of a primary beam intensity was checked by a regular control of standards reflection intensity measurements. The subsequent correction on drifting was performed. The extraction of the integrated intensity I_0 from the measured reflex profile (15 points) I_x was performed using the modified Oatley and French procedure [21]. 1521 non-zero unique reflections of an octant of reciprocal space were measured in eight layers $k = 0$–7 up to $\sin\Theta/\lambda = 1.08$ Å^{-1} in the layer. The intensities were corrected for Lorentz and polarization factors. Absorption corrections ($\mu = 561\,cm^{-1}$) were applied by a numerical integration based on the crystal morphology. 1425 reflections with $I \geqslant 4(\sigma(I))$ were used in the structure determination. The atomic coordinates of Bi from Ref. [20] were used as the initial ones. The scattering factors of the neutral atoms [22] with dispersion corrections for Bi were used. The positions of O and B atoms were located from the difference electron density synthesis calculated after refining of the Bi parameters. The positional and anisotropic thermal parameters of all atoms were refined by a full-matrix block-diagonal least-squares procedure using the modified version of the ORFLS program [23] with the weighting scheme $w = [\sigma^2(F_o) + 0.0006(F_o)^2]^{-1}$. For the other structural calculations the AREN-90 program package [24] was used. The R discrepancy factors (Table 1) were considerably reduced in comparison with $R = 9.7\%$ from the previous study [20]. The final atomic coordinates and equivalent displacement parameters are listed in Table 2, selected interatomic distances and angles are in Table 3. Tables of anisotropic displacement parameters, calculated and observed structure factors have been sent to the Fachinformationzentrum Karlsruhe, Abt. PROKA, 76344 Eggenstein-Leopoldshafen, Germany as supplementary material No. SUP 412831 and can be obtained by contacting the FIZ (quoting the article details and the corresponding SUP number).

Table 2
Atomic parameters and bond valence sums (V) of the $Bi_6B_{10}O_{24}$ crystal structure at 293 K

Atom	x/a	y/b	z/c	B_{eq} (Å^2)	V
Bi(1)	0.45974 (8)	0.25000 (0)	0.81357 (3)	1.17 (1)	2.486/3.009[a]
Bi(2)	0.98519 (5)	0.51686 (7)	0.09560 (2)	1.17 (1)	2.772/3.220[b]
O(1)	0.818 (2)	0.250 (0)	0.9284 (6)	1.5 (3)	2.220
O(2)	0.160 (2)	0.250 (0)	0.8539 (6)	1.2 (3)	2.326
O(3)	0.172 (1)	0.408 (1)	0.9986 (4)	1.4 (2)	2.199
O(4)	0.642 (1)	0.556 (1)	0.2656 (5)	1.7 (2)	1.980
O(5)	0.614 (1)	0.407 (1)	0.1561 (4)	1.7 (2)	2.040
O(6)	0.472 (2)	0.250 (0)	0.9593 (6)	1.7 (3)	2.019
O(7)	0.362 (2)	0.250 (0)	0.0849 (6)	2.1 (3)	1.780
O(8)	0.614 (3)	0.250 (0)	0.2673 (6)	2.3 (4)	1.752
O(9)	0.725 (2)	0.250 (0)	0.0536 (6)	1.3 (3)	1.783
B(1)	0.298 (2)	0.250 (0)	0.0106 (8)	1.7 (5)	3.025
B(2)	0.667 (3)	0.250 (0)	0.9812 (9)	1.1 (4)	2.962
B(3)	0.627 (2)	0.408 (2)	0.2289 (6)	1.4 (3)	3.022
B(4)	0.562 (2)	0.250 (0)	0.110 (1)	1.6 (5)	2.993

$B_{eq} = (\sum(\sqrt{\bar{U}_i^2}))/3$. Standard deviations are given in parentheses.
[a] Bond valence sum for the case of the BiO_3 polyhedron/for the case of the BiO_6 polyhedron.
[b] Bond valence sum for the case of the BiO_4 polyhedron/for the case of the BiO_7 polyhedron.

2.3. High-temperature X-ray powder diffraction study

Thermal expansion of $Bi_3B_5O_{12}$ was studied in air using in situ high-temperature X-ray powder diffraction data collected using the DRON-3 X-ray diffractometer with a high-temperature KRV-1100 camera. The average heating rate was 1.4°C/min for 20–700°C. Unit-cell parameters of the compound at different temperatures were refined by least-squares methods. Temperature dependencies for all unit-cell parameters and cell volume presented in Fig. 1 were described as lines with the following coefficients: $a = 6.529 + 0.000079t$, $b = 7.727 + 0.000098t$, $c = 18.563 + 0.000060t$ Å and $V = 936 + 0.027t$ Å^3. Using these thermal dependencies for orthorhombic a, b and c cell parameters the following main coefficients of tensor of thermal expansion are determined [25] correspondingly: $\alpha_{11} \approx \alpha_{22} = 12$ and $\alpha_{33} = 3 \times 10^{-6}\,°C^{-1}$.

2.4. IR spectrum

IR spectrum in the range of 400–1500 cm^{-1} (Fig. 2) was recorded on a NICOLET NEXUS FT-IR spectrometer using samples prepared as KBr pellets. Vibrational frequencies are given in Table 4. As $Bi_3B_5O_{12}$ has centrosymmetric structure, the complete information about $Bi_3B_5O_{12}$ vibrations is given by data correlation of IR and Raman spectra. The Raman spectrum of $Bi_3B_5O_{12}$ was obtained by us earlier [14].

3. Results and discussion

3.1. Structure description

Cation and anion polyhedra. There are four symmetrically independent B atoms in the asymmetrical unit (Fig. 3). B(2) and B(3) atoms are coordinated by three O atoms in a triangular arrangement, whereas B(1) and B(4) atoms are each tetrahedrally coordinated by four O atoms. The B–O bonds in BO_3 triangles are in the range of 1.34–1.42 Å, and the average $\langle {}^{III}B\text{–}O \rangle$ bond length is 1.38 Å. The B–O bond lengths in BO_4 tetrahedra vary from 1.39 to 1.52 Å, the average $\langle {}^{IV}B\text{–}O \rangle$ bond length being 1.48 Å. These values are close to those from Ref. [30]. The O–B–O angles range from 118° to 123° in the BO_3 triangles and from 104° to 115° in the BO_4 tetrahedra.

Among oxygen atoms the O(2) atom is not bonded to any B atoms. It is coordinated by three Bi atoms in the tops of OBi_3 oxocentered triangle. It should be noted that usually bismuth preferably forms OBi_4 oxocentered tetrahedra [26,27].

There are two symmetrically non-equivalent Bi atoms (Fig. 4) coordinated by six and seven O atoms in $Bi_3B_5O_{12}$. The Bi–O bond lengths are distributed within 2.09–2.75 Å in $Bi(1)O_6$ and within 2.108–2.804 Å in $Bi(2)O_7$ polyhedra (Table 3). The next neighboring oxygen atoms are more than 3.1 Å in BiO_6 and 3.2 Å in BiO_7 apart from Bi atoms. As seen from Table 3 and Fig. 4, Bi atoms have irregular coordination polyhedra. These polyhedra are characteristic of cations with stereoactive lone electron pairs like Bi^{3+}, Pb^{2+} and others [26,27]. In the $Bi(1)O_6$ polyhedron three short bond lengths vary from 2.09 to 2.20 Å with $\langle$Bi–O$\rangle$ equal to 2.16 Å, next neighboring oxygen atom is at 2.71 Å apart from Bi atoms (Table 3). In the $Bi(2)O_7$ polyhedron four short bond lengths are in the range of 2.108–2.331 Å and $\langle$Bi–O$\rangle$ is about 2.20 Å and next neighboring oxygen atom is at 2.785 Å apart from Bi atoms. Taking into account the short Bi–O bonds only the BiO_6 and BiO_7 polyhedra are considered here as

Table 3
B–O and Bi–O bond lengths (Å) and O–B–O (deg) and B–O–B (deg) angles in the $Bi_3B_5O_{12}$ crystal structure

(a) Boron–oxygen

Distances		Angles	
$B^{\square}$(1)–O(7)	1.44 (2)	O(3)–B(1)–O(7)	108 (1)
$B^{\square}$(1)–O(6)	1.48 (2)	O(3)–B(1)–O(3′)	110.2 (6)
$B^{\square}$(1)–O(3) × 2	1.49 (1)	O(3)–B(1)–O(6)	109 (1)
⟨$B^{\square}$(1)–O⟩$_4$	1.48 (2)	O(7)–B(1)–O(6)	113.9 (4)
		⟨O–B(1)–O⟩	110 (3)
B^{A}(2)–O(6)	1.34 (2)	O(1)–B(2)–O(9)	119 (1)
B^{A}(2)–O(1)	1.39 (2)	O(1)–B(2)–O(6)	118 (2)
B^{A}(2)–O(9)	1.40 (2)	O(9)–B(2)–O(6)	123 (2)
⟨B^{A}(2)–O⟩$_3$	1.38 (3)	⟨O–B(2)–O⟩	120.0 (3)
B^{A}(3)–O(4)	1.34 (2)	O(5)–B(3)–O(8)	119.7 (9)
B^{A}(3)–O(5)	1.35 (1)	O(5)–B(3)–O(4)	121 (1)
B^{A}(3)–O(8)	1.42 (2)	O(8)–B(3)–O(4)	119 (3)
⟨B^{A}(3)–O⟩$_3$	1.37 (4)	⟨O–B(3)–O⟩	120 (1)
$B^{\square}$(4)–O(7)	1.39 (2)	O(5)–B(4)–O(9)	103.7 (8)
$B^{\square}$(4)–O(9)	1.50 (2)	O(5)–B(4)–O(5′)	106 (1)
$B^{\square}$(4)–O(5) × 2	1.52 (2)	O(5)–B(4)–O(7)	113.6 (8)
⟨$B^{\square}$(4)–O⟩$_4$	1.48 (6)	O(9)–B(4)–O(7)	115 (2)
		⟨O–B(4)–O⟩	110 (6)
		B(3)–O(5)–B(4)	125 (1)
		B(1)–O(7)–B(4)	127 (2)
		B(3)–O(8)–B(3)′	119 (3)
		B(1)–O(6)–B(2)	122 (4)
		B(2)–O(9)–B(4)	119 (2)
		⟨B–O–B⟩	122 (4)

(b) Bismuth–oxygen

Distances <3.0 Å		Angles	
Bi(1)–O(2)	2.09 (1)	O(2)–Bi(1)–O(4)	87.5 (6)
Bi(1)–O(4) × 2	2.20 (1)	O(4)–Bi(1)–O(4′)	85.7 (9)
Bi(1)–O(6)	2.71 (1)	O(1)–Bi(2)–O(2)	71.5 (4)
Bi(1)–O(5) × 2	2.75 (1)	O(1)–Bi(2)–O(3)	80.6 (7)
⟨Bi(1)–O⟩$_6$	2.4 (3)	O(1)–Bi(2)–O(3′)	84.0 (8)
Bi(2)–O(3)	2.108 (8)	O(2)–Bi(2)–O(3)	146 (1)
Bi(2)–O(2)	2.242 (6)	O(2)–Bi(2)–O(3′)	85.5 (6)
Bi(2)–O(1)	2.258 (6)	O(3)–Bi(2)–O(3′)	73.2 (8)
Bi(2)–O(3′)	2.331 (8)	Bi(2)–O(1)–Bi(2′)	105.83 (6)
Bi(2)–O(9)	2.785 (7)	Bi(1)–O(2)–Bi(2)	123.0 (2)
Bi(2)–O(4)	2.792 (9)	Bi(2)–O(3)–Bi(2′)	106.8 (4)
Bi(2)–O(5)	2.804 (9)		
⟨Bi(2)–O⟩$_7$	2.5 (3)		

BiO_3 irregular trigonal pyramid and BiO_4 irregular tetragonal pyramid, correspondingly (black bonds in Fig. 4). Bi atoms are located in the tops of both pyramids. It is known that lone electron pair is usually located nearly opposite to short bonds. In the both polyhedra short Bi–O bonds link Bi atoms with terminal oxygen atoms in BO_3 and BO_4 polyhedra and with O(2) oxygens that are not bonded to any boron atom.

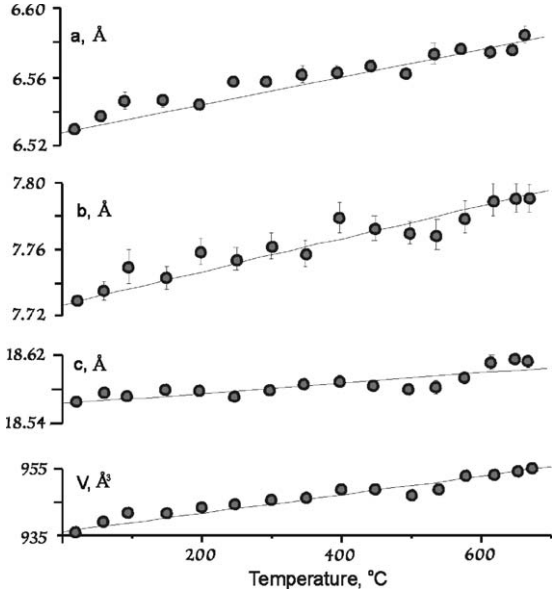

Fig. 1. Temperature dependencies of $Bi_3B_5O_{12}$ unit-cell parameters and cell volume.

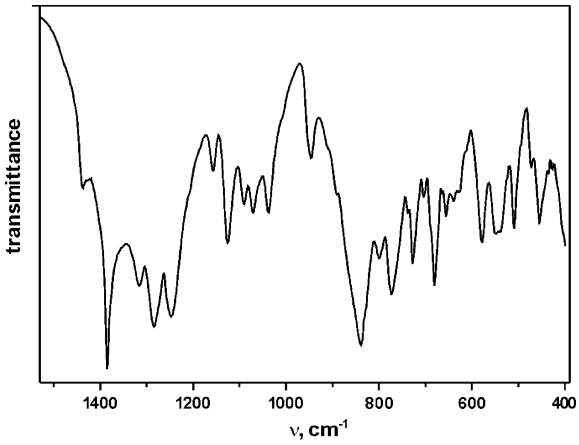

Fig. 2. IR spectrum of $Bi_3B_5O_{12}$.

Bond-valence analysis. Bond-valence sums for atoms in the structure of $Bi_3B_5O_{12}$ were calculated using the bond-valence parameters for B–O and Bi–O bonds from Ref. [28]. The bond-valence sums for B atoms are in the range of 2.962–3.025 v.u. (valence units), for O atoms in the range of 1.752–2.326 v.u. (Table 2). As about Bi atoms, considering BiO_6 and BiO_7 coordination polyhedra the bond-valence sums for Bi atoms are 3.009 and 3.220 v.u., respectively. Taking into account the shortest Bi–O bonds only (threefold and fourfold coordinations) these values are only 2.486 and 2.772 v.u. These values are to a first approximation in a satisfactory agreement with formal atomic valences. Thus, in general, we can consider three and four first-neighbor oxygens as the first coordination spheres of Bi(1) and Bi(2), respectively.

Table 4
The peak frequencies observed on IR and Raman spectra of $Bi_3B_5O_{12}$

IR	Raman [6]	Assignment
427		} $\delta(B_{(4)}-O)$
435	439	
455	452	
473	469	
494	496	} δ(pentaborate anion)
509		
523		} $\delta(B_{(3)}-O)/\delta(B_{(4)}-O)$
538		
550	553	
578	584	
611	616	} $\delta(B_{(4)}-O)$
625	629	
638	638	
657		
681	683	} $\gamma(B_{(3)}-O)$
690	699	
704	734	
728		
739		
773	766	} $\nu_s(B_{(4)}-O)$
800		

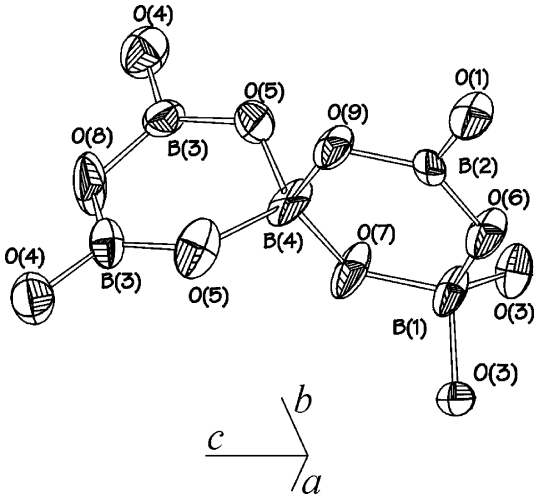

Fig. 3. B–O pentaborate group consisting of two BO_4 tetrahedra and three BO_3 triangles. The thermal ellipsoids are scaled to enclose a probability density of 50%.

Borate anion: structure and geometry. The $[B_5O_{11}]^{7-}$ isolated anion (Fig. 3) is composed of two tetrahedra and three triangles. It can be described as consisting of two borate single rings that are condensed via common tetrahedron into a double ring known as pentaborate group via common tetrahedron: a triborate group formed by a BO_4 tetrahedron and two BO_3 triangles and another triborate group consisting of two BO_4 tetrahedra and a BO_3 triangle. Using the designations suggested in Ref. [29,30], the BO_4 tetrahedron is denoted as T or $\square$ and the BO_3 triangle is denoted as Δ. Thus, according to Heller's nomenclature [29], both triborate groups are symbolized as 3: $2\Delta+T$ and 3: $\Delta+2T$,

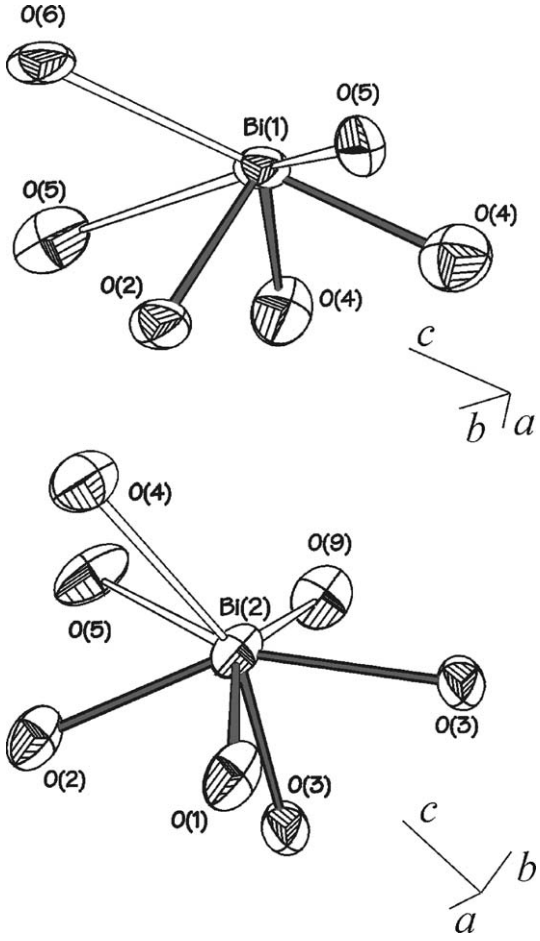

Fig. 4. BiO_6 and BiO_7 polyhedra.

respectively. The pentaborate group contains: 5: $3\Delta+2T$. Burns et al. [30] suggested additional descriptions of the connectivity of borate polyhedra in any subunit. The $\langle\ \rangle$ delimiters indicate that borate polyhedra form a ring and '-' or '=' signs between two rings indicate that they share one or two polyhedra, respectively. Thus, the symbols of the triborate groups are $\langle 2\Delta\square\rangle$ and $\langle\Delta 2\square\rangle$, respectively, and the pentaborate group contains 5B: $\langle 2\Delta\square\rangle$-$\langle\Delta 2\square\rangle$.

The average B–O bond lengths and angles in the BO_4 and BO_3 groups (Table 3) are typical for well-refined structures [30,17], although individual bonds are scattered greatly as noted by Filatov and Bubnova [17]. The B–O–B angles between BO_3 and BO_4 polyhedra within a pentaborate group are scattered from 119° to 127° (Table 3). Oxygen atoms appear in three different environments by boron atoms. So there are six types of B–O bonds in the structure: B^{Δ}–$^{\square}O^{\Delta}$, B^{Δ}–$^{\Delta}O^{\Delta}$, $B^{\square}$–$^{\square}O^{\square}$, $B^{\square}$–$^{\square}O^{\Delta}$, B^{Δ}–$^{\Delta}O$, $B^{\square}$–$^{\square}O$, where B^{Δ} and $B^{\square}$ represent B atoms in threefold and fourfold coordinations, respectively, and $^{\Delta}O^{\Delta}$, $^{\square}O^{\square}$, $^{\square}O^{\Delta}$, $^{\Delta}O$, $^{\square}O$ are oxygen atoms that are bridging between BO_3 and BO_3 groups, BO_4 and BO_4 groups, and BO_3 and

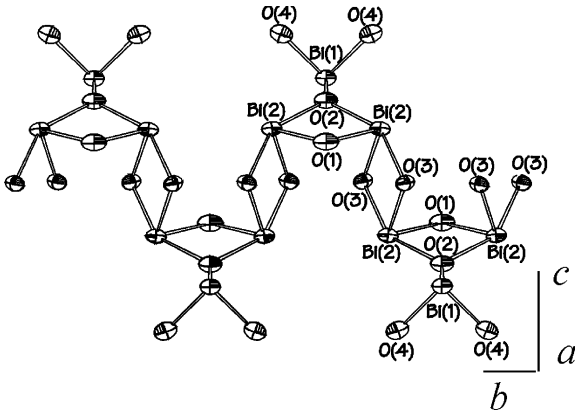

Fig. 5. Zigzag chain of $Bi(2)O_4$ and $Bi(1)O_3$ polyhedra projected along *b*-axis.

BO_4 groups, and non-bridging O atoms of BO_3 and BO_4, respectively. The average $\langle B^{\square}-^{\square}O^{\square}\rangle$ bond length of 1.42 Å is shorter than the $\langle B^{\square}-^{\square}O^{\Delta}\rangle$ length of 1.51 Å, and the $\langle B^{\Delta}-^{\Delta}O^{\Delta}\rangle$ bond length (1.42 Å) is longer than the $\langle B^{\Delta}-^{\Delta}O^{\square}\rangle$ bond length (1.36 Å). These values are very close to those found in [17].

Structure description. The structure consists of isolated polyanions $[B_2^{IV}B_3^{III}O_{11}]^{7-}$, Bi^{3+} cations and O^{2-} anions, not bonded to any boron–oxygen group and situated in the centers of isolated OBi_3 triangles [20]. The BiO_4 polyhedra are shared by O(3)–O(3)′ and O(1)–O(2) oxygen edges to form zigzag chains along *b*-axis with the zigzag along *c*-axis. The BiO_3 polyhedra are connected to these chains by sharing O(2) oxygens (Figs. 5 and 6a). These chains alternate with $(B_5O_{11})^{7-}$ isolated anions by sharing common oxygens to form thick layers extended in *ab* plane (Fig. 6b). The sheets are connected to each other due to weak Bi(2)–O(4) bonds of $Bi(2)O_7$ polyhedra. It should be noted that a perfect cleavage corresponds to these sheets and an imperfect cleavage corresponds to zigzag chains of Bi–O polyhedra.

3.2. Thermal expansion

The compound shows highly anisotropic thermal expansion (Fig. 1): directions of maximum coefficients of thermal expansion tensor, $\alpha_{11}\approx\alpha_{22}=12\times10^{-6}\,^{\circ}C^{-1}$, are along *a*- and *b*-axis and the minimum one, $\alpha_{33}=3\times10^{-6}\,^{\circ}C^{-1}$, is along *c*-axis. Maximum thermal expansion occurs in the directions parallel to sheets in *ab* plane (Fig. 6). The structure practically does not extend perpendicular to the sheets along *c*-axis. The anisotropy of thermal expansion may be caused by a straightening of the Bi–O zigzag chains along *b*-axis and their simultaneous contraction with the decreasing of their zigzag along *c*-axis. It occurs likely due to changing of Bi–O–Bi and O–BI–O angles. It should be noted that the maximum axes of Bi^{3+} and O^{2-} ellipsoids of thermal vibrations are situated along *b*-axis (Fig. 5).

The volume $\alpha_V=27\times10^{-6}\,^{\circ}C^{-1}$ and average linear $\alpha=\alpha_V/3=9\times10^{-6}\,^{\circ}C^{-1}$ coefficients of thermal expansion are compared with the other Bi^{3+} borates: $\alpha_V=34\times10^{-6}\,^{\circ}C^{-1}$ for BiB_3O_6 [11] and $41\times10^{-6}\,^{\circ}C^{-1}$ for $Bi_4B_2O_9$ [12]. At the same time, volume thermal expansion of alkali metal borates ($\alpha_V\approx60\times10^{-6}\,^{\circ}C^{-1}$ [17]) is about twice greater than Bi^{3+} borates expansion.

3.3. Vibrational spectra

It is known [14] that the vibrations of bismuth–oxygen polyhedra are observed below 450–500 cm^{-1}. Thus, the lines apparent in IR and Raman spectra of $Bi_3B_5O_{12}$ in the range of 450–1500 cm^{-1} (Fig. 2, Table 4) are caused by $[B_5O_{11}]^{7-}$ anion vibrations. As it can be seen from Table 4 in IR and Raman spectra of $Bi_3B_5O_{12}$ the vibrations of $[BO_3]$ and $[BO_4]$ groups are observed. According to data from Refs. [31,32], the fundamental vibrations of $[BO_4]$ groups are expected in the ranges of $\nu_s\sim740$–$890\,cm^{-1}$, $\delta\sim400$–$600\,cm^{-1}$, $\nu_{as}\sim1000$–$1150\,cm^{-1}$ and $\delta\sim600\,cm^{-1}$. Four fundamental vibrations attributed to $[BO_3]$ groups are observed in the following ranges: $\nu_s\sim850$–$960\,cm^{-1}$, $\gamma\sim650$–$800\,cm^{-1}$, $\nu_{as}\sim1100$–$1450\,cm^{-1}$ and $\delta\sim500$–$600\,cm^{-1}$ [31,32]. A low site symmetry of $[BO_4]$ and $[BO_3]$ groups in $Bi_3B_5O_{12}$ crystal structure results in the split of these vibrations. Therefore $Bi_3B_5O_{12}$ IR-spectrum demonstrates a large number of lines in these ranges (Fig. 2).

$Bi_3B_5O_{12}$ IR-spectrum is somewhat alike the alkali pentaborates spectra [33,34]. The pentaborate anion $[B_5O_{10}]^{5-}$ ($[B_5O_6(OH)_4]^{-}$—in hydrated borates) is build up from two triborate rings consisting of two BO_3 triangles and one BO_4 tetrahedra. This corresponds completely to the structure of one ring of $[B_5O_{11}]^{7-}$ anion in $Bi_3B_5O_{12}$ (Fig. 3). The normal coordinate analysis of $[B_5O_{10}]^{5-}$ anion (within the framework of D_{2d} symmetry) showed [33] that the deformation vibrations of pentaborate anion occur near 500 cm^{-1}. The totally symmetrical and asymmetrical vibrations were observed in the ranges of 950–1025 and 1350 cm^{-1}, accordingly. The presence of additional oxygen in $[B_5O_{11}]^{7-}$ anion in $Bi_3B_5O_{12}$ structure lowers pentaborate anion symmetry up to D_{2h} resulting in the split of these vibrations. Ulexite ($NaCaB_5O_{10}$ $8H_2O$) IR and Raman spectra can serve as the proof of this fact [34]. Pentaborate anion $[B_5O_6(OH)_6]^{3-}$ in ulexite consists of two triborate rings containing one BO_3 and two BO_4 polyhedra, that corresponds to the second ring of $[B_5O_{11}]^{7-}$ anion in $Bi_3B_5O_{12}$ (Fig. 3). That is why on the base of [31–34] it is possible to give interpretation of the $Bi_3B_5O_{12}$ vibrational spectra (Table 4).

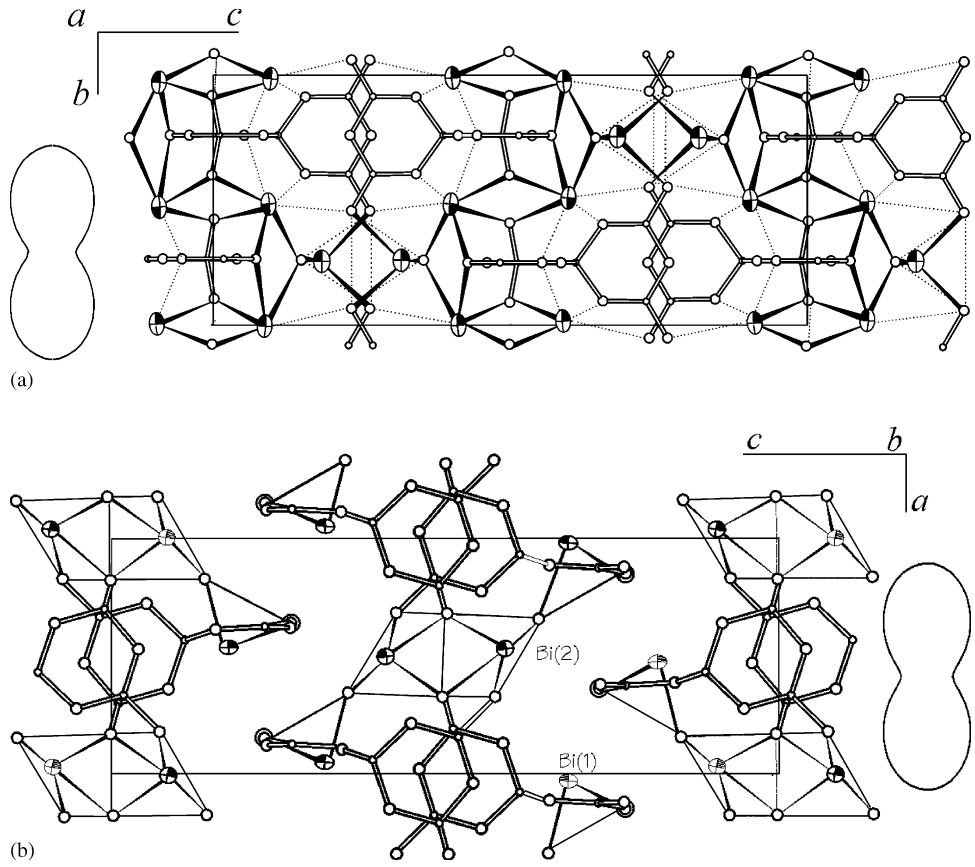

Fig. 6. Correlation between the pole figure for the thermal expansion coefficients and the layered structure of $Bi_3B_5O_{12}$ projected onto *bc* (a) and *ac* (b) plane. Layers are parallel to *ab* plane in the structure of $Bi_3B_5O_{12}$. Ellipsoids for the Bi atoms are drawn at the 50% probability level. Atom labels of BiO chain are given in Fig. 5.

4. Conclusions

The $Bi_3B_5O_{12}$ crystal structure was refined in anisotropic approximation: the esds of atomic parameters were lowered in about 10 times in comparison with the first study [20]. The structure is considered here as a layered one. BiO_6 and BiO_7 polyhedra are extremely irregular due to stereoactive lone electron pairs of Bi^{3+} cations. Using only the shortest Bi–O bonds we described the BiO_6 and BiO_7 polyhedra as irregular BiO_3 trigonal and BiO_4 tetragonal pyramids which are linked by edges to form flexible chains. These zigzag chains alternate with isolated anions $(B_5O_{11})^{7-}$ to form sheets extended in *ab* plane.

Maximum thermal expansion occur parallel to the sheets and the structure practically does not extend in the direction perpendicular to the sheets likely due to a straightening of the Bi–O polyhedra zigzag chains along *b*-axis and decreasing of their zigzag along *c*-axis. A perfect cleavage (001) corresponds to these sheets and an imperfect cleavage (100) is parallel to the zigzag chains of Bi–O polyhedra. Thus, the strongest bonding in the structure of $Bi_3B_5O_{12}$ is realized in the Bi–O chains. The $Bi_3B_5O_{12}$ IR and Raman spectra in the range of 450–1500 cm^{-1} are interpreted in terms of $[B_5BO_{11}]^{7-}$ anion vibrations.

Acknowledgments

This research has been supported by the Russian Foundation for Basic Research, grants 02-03-32842 (S.K.F., Yu.F.Sh., R.S.B., and N.A.S.), 02-03-33280 (A.V.E., and Yu.F.K.) and 03-03-06623 (N.A.S.).

References

[1] C.T. Chen, B.C. Wu, A.D. Jiang, G.M. You, Sci. Sin. B 28 (1985) 235.
[2] C. Chen, Y. Wu, R. Li, J. Cryst. Growth 99 (1990) 790.
[3] Y. Wu, T. Sasaki, S. Nakai, A. Yokotani, H. Tang, C. Chen, Appl. Phys. Lett. 62 (1993) 2614.
[4] Y. Mori, I. Kuroda, S. Nakajinia, et al., Appl. Phys. Lett. 67 (1995) 1818.
[5] M. Iwai, T. Kobayashi, H. Furuya, et al., Jpn. J. Appl. Phys. 36 (1997) L276.
[6] M. Touboul, E. Betourne, Solid State Ion. 63–65 (1993) 340.
[7] H. Hellwig, J. Liebertz, L. Bohaty, J. Appl. Phys. 88 (1) (2000) 240.

[8] B. Teng, J. Wang, Z. Wang, H. Jiang, X. Hu, R. Song, H. Liu, Y. Liu, J. Wei, Z. Shao, J. Cryst. Growth 224 (2001) 280–283.
[9] C. Du, Z. Wang, J. Liu, X. Xu, B. Teng, K. Fu, J. Wang, H. Jiang, Y. Liu, Z. Shao, Appl. Phys. B 73 (2001) 215–217.
[10] M. Muehlberg, M. Burianek, H. Edongue, C. Poetsch, J. Cryst. Growth 237–239 (2002) 740–744.
[11] P. Becker, L. Bohaty, Cryst. Res. Technol. 36 (2001) 1175–1180.
[12] S.K. Filatov, J.V. Alexandrova, Ju.F. Shepelev, R.S. Bubnova, VIII National Meeting on Hightemperature Chemistry of Silicates and Oxides, St. Petersburg, 19–21 November, 2002, p. 267.
[13] P. Becker, P. Held, Cryst. Res. Technol. 36 (2001) 1353–1356.
[14] A.V. Egorysheva, V.I. Burkov, V.S. Gorelick, Yu.F. Kargin, V.V. Koltashev, B.G. Plotnichenko, Fiz. Tverd. Tela 43(9) (2001) 1590–1593 (Phys. Solid State 43 (2001) 1655–1658, Engl. transl.)
[15] A.V. Egorysheva, A.S. Konisheva, Yu.F. Kargin, J.E. Gorbunova, Yu.N. Mikhailov, Zh. Neorg. Khim. 47 (2002) 1961–1965 (Russ. J. Inorg. Chem. 47 1804–1808 (2002), Engl. transl.)
[16] G. Blasse, E.W.J.L. Oomen, J. Liebertz, Phys. Stat. Sol. (b) 137 (1986) K77.
[17] S.K. Filatov, R.S. Bubnova, Phys. Chem. Glasses 41 (5) (2000) 216–224.
[18] E.M. Levin, C.L. McDaniel, J. Am. Ceram. Soc. 45 (1962) 355–360.
[19] J. Liebertz, Prog. Cryst. Growth Charact. 6 (1983) 361.
[20] A. Vegas, F.H. Cano, S. Garsia-Blanco, J. Solid State Chem. 17 (1976) 151–155.
[21] S. Oatley, S. French, Acta Crystallogr. A 38 (1982) 537.
[22] A.J.C. Wilson (Ed.), International Tables for X-ray Crystallography, Vol. C., Kluwer Academic Publishers, Dordrecht/Boston/London, 1995, p. 477.
[23] W.R. Busing, K.O. Martin, H.A. Levy, Osk Ridge Nat. Labor. Report ornl-TM-306, Tenesse, 1962.
[24] V.I. Andrianov, Kristallografiya 32 (1) (1987) 228.
[25] S.K. Filatov, Russ. Chem. Rev. 61 (11) (1992) 1983–1991.
[26] S.V. Krivovichev, S.K. Filatov, Acta Crystallogr. B 55 (1999) 664–676.
[27] S.V. Krivovichev, S.K. Filatov, Crystal chemistry of minerals and inorganic compounds with complexes of anion centered tetrahedra, St. Petersburg State University, St. Petersburg, 2001, p. 46.
[28] N.E. Brese, M. O'Keeffe, Acta Crystallogr. B 47 (1991) 192.
[29] G. Heller, Top. Curr. Chem. 131 (1986) 39.
[30] P.S. Burns, J.D. Grice, F.C. Hawthorne, Can. Miner. 22 (1995) 1131.
[31] C.E. Weir, R.A. Schroeder, J. Res. NBS 68 A (5) (1964) 465–487.
[32] L. Jun, X. Shuping, G. Shiyang, Spectrochimica Acta 51 A (4) (1995) 519–532.
[33] R. Janda, G. Heller, Spectrochimica Acta 36 A (11) (1980) 997–1001.
[34] V. Devaragan, E. Gräfe, E. Funck, Spectrochimica Acta 32 A (5) (1976) 1225–1233.